Werk

Jahr: 1977
Kollektion: fid.geo
Signatur: 8 Z NAT 2148:
Digitalisiert: Niedersächsische Staats- und Universitätsbibliothek Göttingen
Werk Id: PPN1015067948_0043
PURL: http://resolver.sub.uni-goettingen.de/purl?PPN1015067948_0043

LOG Id: LOG_0095
LOG Titel: Attenuation coefficients of acoustic normal modes in shallow water
LOG Typ: article

Übergeordnetes Werk

Werk Id: PPN1015067948
PURL: http://resolver.sub.uni-goettingen.de/purl?PPN1015067948
OPAC: http://opac.sub.uni-goettingen.de/DB=1/PPN?PPN=1015067948

Contact

Niedersächsische Staats- und Universitätsbibliothek Göttingen
Georg-August-Universität Göttingen
Platz der Göttinger Sieben 1
37073 Göttingen
Germany
Email: gdz@sub.uni-goettingen.de

J. Geophys. 43, 569–580, 1977

Journal of Geophysics

Attenuation Coefficients of Acoustic Normal Modes in Shallow Water

H.-H. Essen

Institut für Geophysik der Universität Hamburg, Bundesstr. 55, D-2000 Hamburg 13, Federal Republic of Germany

Abstract. Transmission loss of acoustic energy in shallow water is mostly affected by the sea floor. Normal-mode attenuation is computed as based on the absorption and generation of low-velocity shear waves within the ocean sediments. Results from a summer and winter sound-velocity profile and from a homogeneous and a layered sedimentary halfspace are compared. Two conclusions may be drawn: a) Shear-wave absorption effects normal-mode attenuation remarkably; b) the layering in shear-wave velocities disturbs the frequency dependance of mode-attenuation coefficients. Frequency bands of low and high attenuation are found.

Key words: Acoustic normal modes – Transmission loss – Ocean sediments: absorption and low-velocity shear waves.

1. Introduction

In the last 30 years acoustic normal-mode propagation was investigated in a number of papers. The first theoretical and experimental results from mode theory in shallow water were published by Pekeris (1948). He succeeded in explaining the main features of observed seismograms. Kind (1970) as well compared observed and synthetic seismograms and stated the absence of shear waves in ocean sediments. Beside these experiments with explosives continuous wave (=CW) sources were used e.g. by Tolstoy (1958) and Ferris (1972) in shallow-water areas, and by Guthrie et al. (1960) in the deep ocean. Normal-mode theory was applied to sound propagation in the SOFAR-channel by Tolstoy and May (1960).

Theoretically predicted normal-mode properties such as group velocity, horizontal, and vertical wavenumbers are experimentally verified. On the other hand little is known about mode attenuation. Apart from geometrical (cylindrical) spreading other mechanisms must be considered in order to explain experimental results, e.g. reflection and scattering losses, cf. Weston (1963).

In the present paper only mode attenuation due to reflection losses at an sedimentary bottom are investigated. Transmission loss is caused by transforming acoustic energy into low-velocity shear waves and absorption of compressional and shear waves in the sediment. Absorption of compressional waves was first considered by Kornhauser and Raney (1955). Ingenito (1973) applied similar computations to measured mode attenuation in a shallow-water area of the Gulf of Mexico.

It is shown that compressional wave absorption and generation of shear waves in a homogeneous sedimentary sea floor yield comparable mode attenuation. The sound velocity profile of the shallow-water area is of importance, attenuation in summer is greater than in winter.

With regard to undisturbed mode propagation the layering of the sea floor is of small influence. This is found from theory and is in agreement with measurements. But as a result of this paper it is shown that due to mode attenuation the layering of the sedimentary sea floor can not be neglected.

2. Lossless Normal-Mode Propagation

In shallow-water areas of approximately constant depth sound propagation is best presented by a superposition of normal modes. The two-fluid model, first treated by Pekeris (1948), turned out to yield good agreement between computed and measured mode characteristics, propagation velocity and vertical amplitude distributions (Ferris, 1972; Essen et al., 1975). In this model a water layer of constant depth is overlying a sedimentary halfspace of constant density and sound velocity. The density of the water layer is constant as well, but the sound velocity may depend on depth. The geometry is shown in Figure 1.

Normal-mode theory assumes total reflection at the sea surface and floor. Due to the non-rigid sea bottom only a finite number of modes is trapped within the wave guide.

Considering a point source of circular frequency ω the acoustic pressure at long distance r is found to be,

$$p(r, x_3, t) = r^{-\frac{1}{2}} \sum_{n=1}^{N(\omega)} P_n \varphi_n(x_3) \exp(i(k_n r - \omega t)) \tag{1}$$

x_3 = depth of receiver,
k_n = horizontal wavenumber,
$n = 1, \ldots, N(\omega)$ = number of mode.

The complex amplitudes P_n depend on source characteristics and wave-guide model. The mode functions $\varphi_n(x_3)$ oscillate within the water layer and decrease exponentially within the sedimental halfspace,

$$\varphi_n(x_3) = \begin{cases} \varphi_n^w(x_3) & \text{for } 0 \geqq x_3 \geqq -h \\ \varphi_n^b(x_3) & \text{for } -h \geqq x_3. \end{cases}$$

Due to the x_3-dependend sound velocity in the water layer $\varphi_n^w(x_3)$ must be computed numerically, while $\varphi_n^b(x_3)$ is given explicitely,

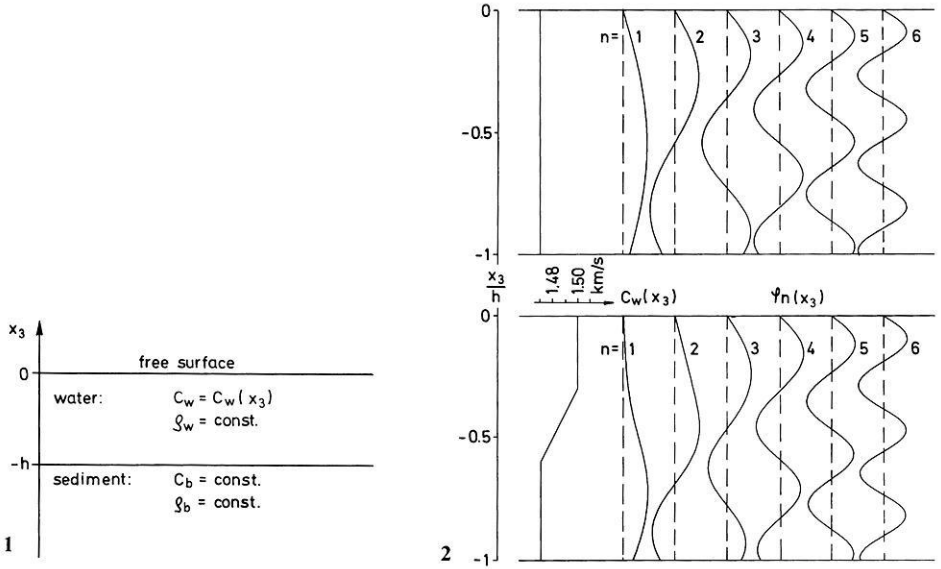

Fig. 1. Geometry of a 2-layer model. c sound velocity, ρ density

Fig. 2. Normal-mode functions $\varphi_n(x_3)$; *upper part:* constant (winter) sound-velocity profile; *lower part:* typical summer profile; dimensionless frequency: $\frac{\omega h}{c_0}=35$; $h=$water depth, $c_0=1.5\,\mathrm{km}\cdot\mathrm{s}^{-1}$; sediment parameters: compressional-wave velocity $c_b=1.167\cdot c_0$, density $\rho_b=1.9\cdot\rho_w$ ($\rho_w=$density of water)

$$\varphi_n^{w\,\|}(x_3)+\left(\frac{\omega^2}{c_w^2(x_3)}-k_n^2\right)\varphi_n^w(x_3)=0$$

$$\varphi_n^b(x_3)=\alpha_n\exp\left(\sqrt{k_n^2-\frac{\omega^2}{c_b^2}}\cdot x_3\right) \tag{2}$$

$c_w, c_b=$compressional-wave velocities of water (w) and sediment (b),
$a_n=$arbitrary amplitudes.

The pressure free surface and continuity of pressure and vertical particle velocity at the sea floor yield the boundary conditions,

$$\varphi_n^w(0)=0 \tag{3}$$

and,

$$\varphi_n^w(-h)=\varphi_n^b(-h)$$

$$\frac{1}{\rho_w}\varphi_n^{w\,|}(-h)=\frac{1}{\rho_b}\varphi_n^{b\,|}(-h).$$

With help of (2) one obtains,

$$\varphi_n^{w\,|}(-h)-\beta_n\varphi_n^w(-h)=0 \tag{4}$$

with,

$$\beta_n = \frac{\rho_w}{\rho_b}\sqrt{k_n^2 - \frac{\omega^2}{c_b^2}}.$$

The horizontal wavenumbers k_n are eigenvalues of the equations (2) with the boundary conditions (3) and (4). For arbitrary sound-velocity profiles this problem has to be solved numerically.

In Figure 2 normal-mode functions are presented for a fixed dimensionless frequency $\frac{\omega h}{c_0}$. The sediment parameters are chosen from typical North-Sea conditions (Essen et al., 1973). The upper part refers to constant sound velocity within the water layer. Due to mixing by surface waves this may be assumed for water depths less than 20 m. During winter, when there is no temperature gradient, constant sound velocity is a good approximation for deeper areas as well. The lower part refers to an idealized summer profile of a 60 m-deep area of the North Sea (Wille et al., 1973). Here, the energy of the first modes is concentrated on the lower part of the ocean.

3. Reflection Losses at a Homogeneous (Non-Layered) Sea Floor

Though totally reflected the acoustic waves penetrate into the sea floor. This implies that the upper section of the sedimentary halfspace with the thickness of a few acoustic wavelengths has an important influence on normal-mode propagation. Two physical properties of sediments are responsible for reflection losses, absorption and low shear-wave velocity. Due to normal-mode theory small attenuation factors for each mode are introduced, which do not appreciably perturb the eigenvalue problem of the lossless theory.

Absorption can be introduced by assuming a complex compressional-wave velocity (Kornhauser and Raney, 1955),

$$c_b = c_{bR} - i c_{bI} \quad \text{with, } 0 \leqq c_{bI} \ll c_{bR}. \tag{5}$$

Instead of (5) absorption is usually described by a coefficient α_b,

$$\frac{\omega}{c_b} = \frac{\omega}{c_{bR}} + i\alpha_b \tag{6}$$

with,

$$\alpha_b \approx \frac{\omega}{c_{bR}} \cdot \frac{c_{bI}}{c_{bR}}.$$

Direct measurement of bottom absorption show an almost linear increase of the coefficient α_b with frequency (Schirmer, 1971; Hamilton, 1972). Thus, it may be assumed,

$$c_{bI}(\omega) = \text{const.} \tag{7}$$

Sea-floor rigidity is another cause of loss, since it allows the propagation of shear waves. The shear-wave velocity of oceanic sediments can be considered small compared with sound velocity in water. From different experimental

methods shear-wave velocities of 50–500 ms^{-1} were found in water-saturated sediments (Hamilton, 1975).

Now, a sedimentary halfspace is considered with constant shear-wave velocity smaller and compressional-wave velocity higher than the sound velocity of water. In fact, these conditions allow no trapped modes within the water layer as there is no total reflection at the bottom. But normal modes are obtained in the limiting case of zero shear-wave velocity, where the solid halfspace becomes a fluid one. Thus, one expects that for low shear-wave velocities the reflection losses become small.

By allowing for sea-floor rigidity the sedimental halfspace has to be treated as a solid. In this case particle displacements ζ_i $(i=1,2,3)$ and vertical components of stress τ_{i3} are of interest. In agreement with the normal-mode solution (1) and the elastic equations of motion one obtains,

$$\begin{aligned}
\zeta_\alpha &= r^{-\frac{1}{2}} \sum_{n=1}^{N(\omega)} i k_{n\alpha} P_n \left\{ \sigma_n + \frac{1}{k_n} \psi_n^{|} \right\} \exp(i(k_n r - \omega t)) \qquad (\alpha = 1,2) \\
\zeta_3 &= r^{-\frac{1}{2}} \sum_{n=1}^{N(\omega)} P_n \{ \sigma_n^{|} - k_n \psi_n \} \exp(i(k_n r - \omega t))
\end{aligned} \tag{8}$$

and

$$\begin{aligned}
\tau_{\alpha 3} &= r^{-\frac{1}{2}} \rho_b c_s^2 \sum_{n=1}^{N(\omega)} i k_{n\alpha} P_n \left\{ 2\sigma_n^{|} + \left(2k_n^2 - \frac{\omega^2}{c_s^2} \right) \psi_n \right\} \\
&\quad \cdot \exp(i(k_n r - \omega t)) \\
\tau_{33} &= r^{-\frac{1}{2}} \rho_b c_s^2 \sum_{n=1}^{N(\omega)} P_n \left\{ \left(2k_n^2 - \frac{\omega^2}{c_s^2} \right) \sigma_n + 2k_n \psi_n^{|} \right\} \\
&\quad \cdot \exp(i(k_n r - \omega t))
\end{aligned} \tag{9}$$

with

$$\begin{aligned}
&\sigma_n^{||}(x_3) + \left(\frac{\omega^2}{c_b^2} - k_n^2 \right) \sigma_n(x_3) = 0 \\
&\psi_n^{||}(x_3) + \left(\frac{\omega^2}{c_s^2} - k_n^2 \right) \psi_n(x_3) = 0 \\
&c_s = \text{shear-wave velocity.}
\end{aligned} \tag{10}$$

The compressional waves in the sedimentary halfspace are assumed to decrease exponentially while the low velocity shear waves travel to infinity,

$$\begin{aligned}
\sigma_n(x_3) &= A_n \exp\left(\sqrt{k_n^2 - \frac{\omega^2}{c_b^2}} \cdot x_3 \right) \\
\psi_n(x_3) &= B_n \exp\left(-i \sqrt{\frac{\omega^2}{c_s^2} - k_n^2} \cdot x_3 \right).
\end{aligned} \tag{11}$$

The continuity of normal displacements and normal stresses at the fluid-sediment interface yields the boundary condition (4) with,

$$\beta_n = \frac{\rho_w}{\rho_b}\frac{\omega^4}{c_s^4}\frac{\sqrt{k_n^2-\frac{\omega^2}{c_b^2}}}{\left(2k_n^2-\frac{\omega^2}{c_s^2}\right)^2+4ik_n^2\sqrt{k_n^2-\frac{\omega^2}{c_b^2}}\sqrt{\frac{\omega^2}{c_s^2}-k_n^2}} \tag{12}$$

where

$$c_s \ll c_w.$$

A more detailed derivation of (12) is given b Williams and Eby (1962) for a liquid layer of constant sound velocity. They compared computed mode attenuation with measured data from a tank experiment (water layer on rubber).

Beside shear-wave generation shear-wave absorption may be a cause of mode attenuation. In analogy to compressional waves it is assumed,

$$c_s = c_{sR} - ic_{sI}. \tag{13}$$

From the assumption of absorption or generation of low-velocity shear waves within the sedimental halfspace a complex β_n in the boundary condition (4) is obtained. In order to solve the differential equation (2) and boundary conditions (3) and (4) complex functions $\varphi_n(x_3)$ and wavenumbers k_n have to be considered,

$$\begin{aligned} &\varphi_n(x_3) = \varphi_{nR}(x_3) + i\varphi_{nI}(x_3) \\ &k_n = k_{nR} + ik_{nI}, \quad \text{with } k_{nI} \geqq 0. \end{aligned} \tag{14}$$

The imaginary part of the wavenumber yields an attenuation of the horizontally propagating normal-mode solution (1). For computing attenuation the perturbation of the normal-mode solution is considered to be small,

$$\left.\begin{aligned} &\varphi_{nI}(x_3) \approx \varepsilon \cdot \varphi_{nR}(x_3) \\ &k_{nI} \approx \varepsilon \cdot k_{nR} \end{aligned}\right\} \varepsilon \ll 1 \tag{15}$$

where ε depends on the ratios of shear to compressional-wave velocity and imaginary to real part of the bottom-wave velocities.

An equation for k_{nI} is obtained by the following procedure: Equations (14) are inserted into the differential Equation (2) and boundary conditions (3, 4). The real and the imaginary part are separated. The "real" differential equation is multiplied by φ_{nI}, the "imaginary" by φ_{nR}, and both equations are subtracted. The result is integrated with respect to x_3 from $-h$ to 0. With help of the boundary conditions and neglecting terms of higher than first order in ε, one obtains,

$$\beta_{nI}\,\varphi_{nR}^2(-h) + 2k_{nI}\,k_{nR}\int_{-h}^{0}\varphi_{nR}^2(x_3)\,dx_3 = 0$$

with, (16)

$$\beta_{nI} = Im(\beta_n).$$

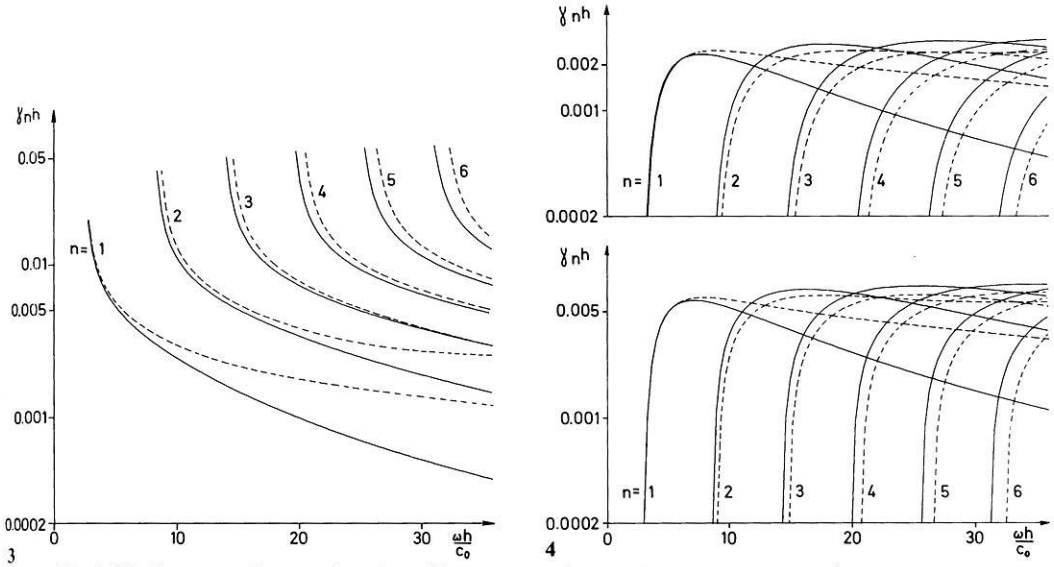

Fig. 3. Mode-attenuation γ_n as function of frequency ω; h water depth, $c_0 = 1.5\,\mathrm{km \cdot s^{-1}}$; ——— winter profile, ------ summer profile; sediment parameters of Figure 2, and, $c_{bI} = 0.005 \cdot c_0$ (imaginary part of compressional-wave velocity)

Fig. 4. Mode attenuation γ_n as function of frequency ω; h water depth, $c_0 = 1.5\,\mathrm{km \cdot s^{-1}}$; ——— winter profile, ------- summer profile; sediment parameters of Figure 2, and, $c_s = c_{sR} - i \cdot c_{sI}$ (complex shear-wave velocity), $c_{sR} = 0.167 \cdot c_0$, $c_{sI} = 0$ (upper part), $c_{sI} = 0.01 \cdot c_0$ (lower part)

This is an implicit equation for k_{nI} as β_{nI} is depending on k_{nI} in a complicated way. The equation will be solved numerically.

Neglecting terms of order ε the function φ_{nR} and wavenumber k_{nR} are solutions of the lossless eigenvalue problem. Figures 3–5 show computed attenuation coefficients of the acoustic intensity,

$$\gamma_n = 2k_{nI}. \tag{17}$$

The dashed lines refer to the constant sound-velocity profile of Figure 2, the dotted lines to the summer profile of Figure 2. In Figure 3 only compressional-wave absorption is considered. The imaginary part of the wave velocity is chosen by,

$$c_{bI} = 0.005 \cdot c_0 \tag{18}$$

with

$$c_0 = 1500\,\mathrm{ms^{-1}}$$

corresponding to a bottom absorption coefficient,

$$\alpha_b = 0.14 \cdot f\,[\mathrm{dB/km}]$$

with, f = acoustic frequency measured in Hz.

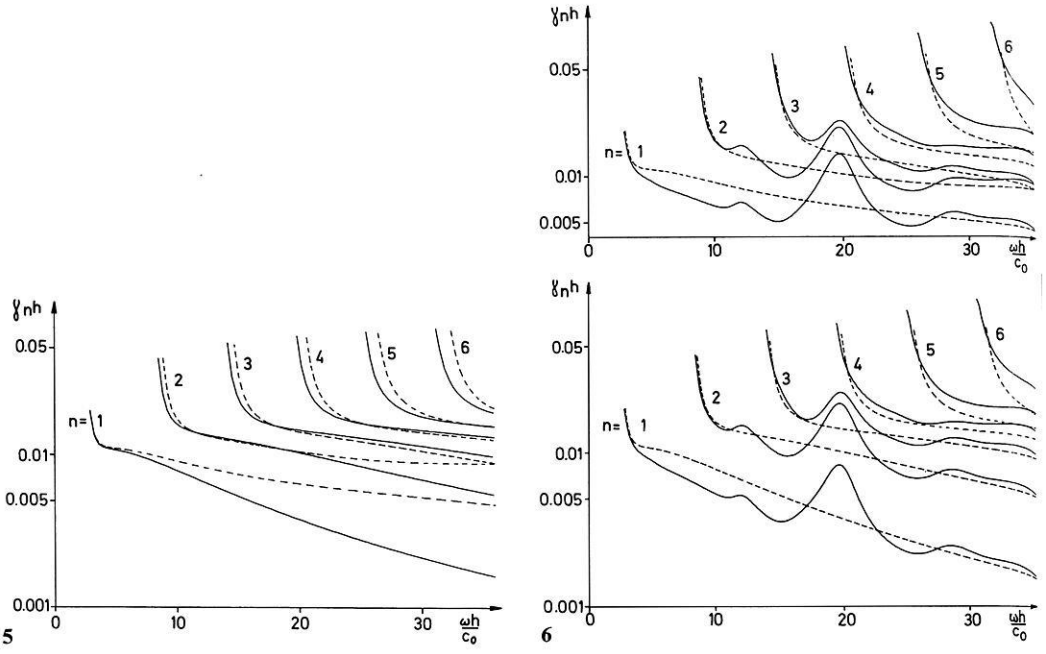

Fig. 5. Mode attenuation γ_n as function of frequency ω; h water depth, $c_0 = 1.5\ \mathrm{km \cdot s^{-1}}$; ——— winter profile, ------- summer profile; sediment parameters of Figure 2, and, $c_{bI} = 0.005 \cdot c_0$ (imaginary part of compressional-wave velocity), $c_{sR} = 0.167 \cdot c_0$ (real part of shear-wave velocity), $c_{sI} = 0.01 \cdot c_0$ (imaginary part of shear-wave velocity)

Fig. 6. Mode attenuation γ_n for a 6-layer model (———) in comparison with the 2-layer values of Figure 5 (-------); *upper part:* summer profile of Figure 2, *lower part:* winter profile of Figure 2; sediment parameters of the 6-layer model

m	h_m/h	ρ_b^m/ρ_w	c_{bR}^m/c_0	c_{bI}^m/c_0	c_{sR}^m/c_0	c_{sI}^m/c_0
1	0.02	1.8	1.133	0.004	0.133	0.008
2	0.02	1.6	1.0	0.002	0.08	0.004
3	0.02	1.9	1.167	0.005	0.167	0.01
4	0.02	1.7	1.067	0.003	0.1	0.006
5	∞	1.9	1.167	0.005	0.167	0.01

h_m = thickness
ρ_b^m = densityof layer m
$c_{bR}^m - ic_{bI}^m$ = compressional-wave velocity
$c_{sR}^m - ic_{sI}^m$ = shear-wave velocity
} $c_0 = 1.5\ \mathrm{km\ s^{-1}}$

This value was found by Schirmer (1971) in sea-floor mud. Measurements in saturated sediments at low frequencies (less than 1 kHz) yield values between $0.08 \cdot f$ and $0.30 \cdot f$ [dB/km] (Hamilton, 1972).

The mode cutoffs are chosen at,

$$\frac{\omega}{k_{nR}} = c_{bR} \quad \text{(for cutoff).} \tag{19}$$

This agrees with the undisturbed mode solutions and is consistent with the assumption (15). The exact cutoff is obtained from (12) by setting $\beta_n = 0$,

$$\left.\begin{aligned} \frac{\omega}{k_{nR}} &= c_{bR}\left(1+\frac{c_{bI}^2}{c_{bR}^2}\right) \\ \frac{k_{nI}}{k_{nR}} &= \frac{c_{bI}}{c_{bR}} \end{aligned}\right\} \quad \text{(for cutoff).} \tag{20}$$

Thus, at cutoff frequencies the mode attenuation becomes equal to the attenuation of compressional waves in the sea floor.

Figure 4 shows the mode attenuation caused by excitation of low-velocity shear waves. The uppper panel refers to lossless shear waves with,

$$\begin{aligned} c_{sR} &= 0.167 \cdot c_0 = 250\ \mathrm{ms}^{-1} \\ c_{sI} &= 0. \end{aligned} \tag{21}$$

Measured shear-wave velocities in water-saturated sediments vary from 50 to over $500\ \mathrm{ms}^{-1}$ (Hamilton, 1975). With an indirect method Janle et al. (1975) found a near-surface velocity of $200\ \mathrm{ms}^{-1}$ in the North Sea. In the cited paper observed elastic bottom motions are assumed to be forced by surface gravity waves.

Shear-wave absorption is even less known than shear-wave velocity. In order to show the influence on mode propagation the attenuation coefficients are computed in Figure 4, lower panel, with,

$$c_{sI} = 0.01 \cdot c_0. \tag{22}$$

In agreement with observations the shear-wave attenuation is assumed proportional to the first power of frequency (Hamilton, 1975). In the same paper it is pointed out that shear-wave attenuation may be of the order of 10 to 20 times larger than compressional wave attenuation, which means even higher than those in (22).

The comparison of Figures 3 and 4 indicates that compressional-wave absorption and shear-wave excitation yield comparable contributions to mode attenuation. The lower part of Figure 4 shows that shear-wave absorption is not neglible. This is of importance because shear-wave absorption of ocean sediments is the most unknown quantity within this investigation.

In Figure 5 the resulting mode attenuation from compressional-wave absorption, shear-wave excitation and absorption is shown. The resulting attenuation coefficients are little smaller than the sum of the contributions from Figures 3 and 4.

The summer profile mainly effects the attenuation of the first two modes $n = 1, 2$. This results from the concentration of mode energy within the lower part of the ocean (cf. Fig. 2).

4. Reflection Losses at a Layered Sea Floor

In this section a $(M+1)$-layer model is regarded. The uppermost layer is the water layer, and the sedimentary halfspace consists of M homogeneous layers of

thickness h_m, density ρ_b^m, compressional-wave velocity c_b^m, and shear-wave velocity c_s^m. The shear-wave velocities of all layers are assumed to be small compared with the sound velocity of the ocean,

$$c_s^m \ll c_w \quad \text{for } m=1, 2, \ldots, M. \tag{23}$$

In order to obtain normal-mode solutions the compressional-wave velocity of the lowest layer (a halfspace) has to exceed the sound velocity of water. The acoustic wave field of the layered elastic halfspace can be described by the particle displacements (8). Within each layer the differential Equations (10) have to be fulfiled, and at the layer boundaries continuity of displacements and normal stresses are required. For the lowest layer the radiation conditions (exponentially decreasing compressional and outgoing shear waves) yield the solutions (11). Assuming arbitrary amplitudes A_n, B_n the vertical amplitude functions σ_n, ψ_n can be continued from the lowest layer up to the upper boundary of the uppermost sedimentary layer. This is done by a matrix formalism similar to that of Haskell (1953). With help of the boundary conditions at the water-sediment interface the amplitudes A_n and B_n are eliminated and β_n [Eq. (4)] is obtained, depending on the transfer matrix only,

$$\beta_n = \frac{\rho_w}{\rho_b^1}\frac{\omega^2}{c_s^{12}} \frac{(T_{22}+k_n T_{32})S_1-(T_{21}+k_n T_{31})S_2}{\left(2k_n T_{41}+\left(2k_n^2-\frac{\omega^2}{c_s^{12}}\right)T_{11}\right)S_2-\left(2k_n T_{42}+\left(2k_n^2-\frac{\omega^2}{c_s^{12}}\right)T_{12}\right)S_1} \tag{24}$$

with

$$S_1 = 2k_n T_{21}+\left(2k_n^2-\frac{\omega^2}{c_s^{12}}\right)T_{31}$$

$$S_2 = 2k_n T_{22}+\left(2k_n^2-\frac{\omega^2}{c_s^{12}}\right)T_{32}$$

where T is the 2×4-transfer matrix,

$$T=\prod_{m=1}^{M-1}(L_m \cdot B_m)\cdot T_M. \tag{25}$$

In this equation T_M is the 2×4 matrix, including the boundary conditions at the lowest interface and the radiation conditions,

$$T_M=\begin{bmatrix} 1 & 0 \\ -i\kappa_b^M & 0 \\ 0 & 1 \\ 0 & -i\kappa_s^M \end{bmatrix} \tag{26}$$

with

$$\kappa_b^m = \begin{cases} \sqrt{\dfrac{\omega^2}{c_b^{m\,2}} - k_n^2} & \text{if } \dfrac{\omega}{c_{bR}^m} > k_{nR} \\ i\sqrt{k_n^2 - \dfrac{\omega^2}{c_b^{m\,2}}} & \text{else} \end{cases}$$

$$\kappa_s^m = \begin{cases} \sqrt{\dfrac{\omega^2}{c_s^{m\,2}} - k_n^2} & \text{if } \dfrac{\omega}{c_{sR}^m} > k_{nR} \\ i\sqrt{k_n^2 - \dfrac{\omega^2}{c_s^{m\,2}}} & \text{else} \end{cases} \tag{27}$$

B_m and L_m are 4×4 matrices which describe the boundary conditions at the layer interfaces and the continuation of the function $\sigma_n(x_3)$ and $\psi_n(x_3)$ through the layers,

$$B_m = \begin{bmatrix} d_m - q_m & 0 & 0 & -q_m/k_n \\ 0 & 1+q_m & k_n(1+q_m-d_m) & 0 \\ 0 & -q_m/k_n & d_m - q_m & 0 \\ k_n(1+q_m-d_m) & 0 & 0 & 1+q_m \end{bmatrix} \tag{28}$$

with

$$d_m = \rho_b^{m+1}/\rho_b^m, \qquad q_m = 2\,\frac{k_n^2}{\omega^2}\,(d_m\, c_s^{m+1\,2} - c_s^{m\,2})$$

and

$$L_m = \begin{bmatrix} \cos(\kappa_b^m h_m) & \sin(\kappa_b^m h_m)/\kappa_b^m & 0 & 0 \\ -\kappa_b^m \sin(\kappa_b^m h_m) & \cos(\kappa_b^m h_m) & 0 & 0 \\ 0 & 0 & \cos(\kappa_s^m h_m) & \sin(\kappa_s^m h_m)/\kappa_s^m \\ 0 & 0 & -\kappa_s^m \sin(\kappa_s^m h_m) & \cos(\kappa_s^m h_m) \end{bmatrix}. \tag{29}$$

The dashed lines in Figure 6 show computed attenuation coefficients for a 6-layer model. The dotted lines refer to a 2-layer model with sediment parameters of the lowest layer of the 6-layer model. Computations are carried out for a constant profile of sound velocity in the ocean and for the summer profile of Figure 2.

It is remarkable that the attenuation coefficients of the layered sea floor no longer decrease monotonously with frequency. As further computations show this is mainly a result of layering in shear-wave velocities. Especially channels of low shear-wave velocity, such as $m=2$ and 4 in Figure 6, effect the frequency dependence of the mode-attenuation coefficients. In agreement with the assumption (15) the layering of the sea floor has no remarkable influence on the mode dispersion.

5. Conclusions

A 2-layer fluid model is a good approximation for lossless mode theory. Even for order-of-magnitude estimations of attenuation the 2-layer model yields

useful results (Ingenito, 1973). But, as shown in Figure 6, the sea-floor layering must be regarded for more accurate investigations. Schirmer (1971) observed a layering of compressional-wave velocities in the upper few meters of ocean sediments. On the other hand nothing is known about shear-wave layering, which mainly effects the frequency dependence of mode attenuation. Therefore the computation of exact mode-attenuation coefficients is not possible. But the theoretical results may help to understand observed transmission loss in shallow-water acoustics.

Acknowledgements. This work was supported by the Deutsche Forschungsgemeinschaft, Sonderforschungsbereich 94, Meeresforschung.

References

Essen, H.-H., Hirschleber, H.B., Siebert, J.: Geschwindigkeits- und Dämpfungsmessungen an Sedimenten der Nordsee. Z. Geophys. **39**, 833–854, 1973

Essen, H.-H., Kebe, H.-W., Siebert, J.: Acoustic normal modes generated by explosive sources, J. Geophys. **41**, 111–122, 1975

Ferris, R.H.: Comparison of measured and calculated normal-mode amplitude functions for acoustic waves in shallow water. J. Acoust. Soc. Am. **48**, 981–988, 1972

Guthrie, A.N., Tolstoy, I., Shaffer, J.: Propagation of low-frequency CW sound signals in the deep ocean. J. Acoust. Soc. Am. **32**, 645–647, 1960

Hamilton, E.L.: Compressional-wave attenuation in marine sediments. Geophysics **37**, 620–646, 1972

Hamilton, E.L.: Acoustic properties of the sea floor: a review. Conference Proceedings 17, Saclantcen, 1975

Haskell, N.A.: The dispersion of surface waves on multilayered media. Bull. Seismol. Soc. Am. **43**, 17–34, 1953

Ingenito, F.: Measurements of mode attenuation coefficients in shallow water. J. Acoust, Soc. Am. **53**, 858–863, 1973

Janle, P., Rudloff, R., Schmalfeldt, B., Szelwis, R.: Seegangserzwungene elastische Bewegungen des Nordseebodens. J. Geophys. **41**, 475–489, 1975

Kind, R.: Auswertung seeseismischer Messungen mit einer digitalen Methode unter Anwendung der Theorie der Schallwellenausbreitung im Flachwasser. Z. Geophys. **36**, 549–567, 1970

Kornhauser, E.T., Raney, W.P.: Attenuation in shallow water propagation due to an absorbing bottom. J. Acoust. Soc. Am. **27**, 689–692, 1955

Pekeris, C.L.: Theory of propagation of explosive sound in shallow water. Geol. Soc. Am. Mem. **27**, 43–70, 1948

Schirmer, F.: Eine Untersuchung akustischer Eigenschaften von Sedimenten der Nord- und Ostsee. Dissertation, Universität Hamburg, 1971

Tolstoy, I.: Shallow water test of the theory of layered wave guides. J. Acoust. Soc. Am. **30**, 348–361, 1958

Tolstoy, I., May, J.: A numerical solution for the problem of long-range sound propagation in continuously stratified media, with application to the deep ocean. J. Acoust. Soc. Am. **32**, 655–660, 1960

Weston, D.E.: Propagation of sound in shallow-water. J. Brit. I.R.E. **26**, 329–337, 1963

Wille, P., Thiele, R., Schunk, E.: Shallow-water sound attenuation in a standard area. J. Acoust. Soc. Am. **54**, 1708–1726, 1973

Williams, A.O., Eby, R.B.: Acoustic attenuation in a liquid layer over a "slow" viscoelastic solid. J. Acoust. Soc. Am. **34**, 836–843, 1962

Received January 24, 1977; Revised Version March 11, 1977